A Highly Compact Low-Profile Beam-Switching Transmitarray Antenna for ISM-Band Applications

S. H. Ramazannia Tuloti, Adam Lamecki, *Senior Member, IEEE*, and Michal Mrozowski, *Fellow, IEEE*

***Abstract*—This leter presents a novel, very low-profile transmitarray antenna (TA) designed specifically for applications in the 24 GHz Industrial, Scientific, and Medical (ISM) band. The design innovation lies in embedding the switchable feed antenna into the beam-focusing surface and adding a reflector, which effectively halves the antenna's size in the boresight direction. This compact antenna allows for easy beam switching through the use of microswitches, making it well suited for vehicular radar applications. A TA consisting of 829 units with an *F/D* ratio of 0.5 has been successfully engineered and fabricated for operation at 24.125 GHz. Notably, the antenna exhibits beam-switching capabilities at various angles, including 8°, 16°, and 24° in the negative *X*-axis direction and 8°, 16°, 24°, and 32° in the positive *X*-axis direction, in addition to the boresight direction. The maximum measured gain of the antenna is 19.85 dBi, and it can achieve a tilt of 32° with a gain reduction of approximately 3.52 dB compared to the boresight direction.**

***Index Terms*—Beam switching, compact structure, low profile design, patch antenna, transmitarray antennas.**

I. Introduction

In RECENT years, transmitarray antennas (TAs) have gained significant traction in communication systems due to their flexibility in beam steering [1], [2], [3], [4], [5]. Traditional TAs, which comprise a separate feed antenna and beam-focusing surface, often suffer from increased dimensions and manufacturing complexities [6], [7], [8], [9], [10]. Our study addresses these challenges by integrating the feed antenna into the beam-focusing surface and adding a reflector, simplifying the structure and reducing the overall profile.

The integration of a separate feed antenna, such as a horn antenna, leads to increased manufacturing complexities and a larger antenna profile [11], [12]. To overcome these challenges, this paper aims to simplify the construction process and reduce the dimensions of TAs. The key innovation is the integration of the feed antenna into the beam-focusing surface and the addition of a reflector plate to eliminate the necessity for a complex supporting structure. Also, as the reflector can be part of the vehicle or the instrument on which the antenna will be placed, this design will be simple in processing and installation.

Received 19 July 2024; revised 11 October 2024; accepted 11 November 2024. Date of publication 21 November 2024; date of current version 5 February 2025. This work was supported by the Polish National Science Centre under Contract UMO-2019/33/B/ST7/00889. *(Corresponding author: S. H. Ramazannia Tuloti.)*

The authors are with the Faculty of Electronics, Telecommunications, and Informatics, Gdansk University of Technology, 80-233 Gdansk, Poland (e-mail: h.ramazannia@pg.edu.pl; adam.lamecki@ieee.org; m.mrozowski@ieee.org).

Digital Object Identifier 10.1109/LAWP.2024.3504373

To achieve beam scanning/switching in TAs, two predominant approaches are typically employed. The first strategy utilizes active devices, such as PIN diodes in the antenna's unit cells to adjust the phase of each cell, facilitating beam tilting [13], [14], [15], [16], [17], [18]. However, this method introduces significant complexities in the design and construction of the feeding network, often requiring a dedicated processor for precise phase control [19], [20], [21]. The second approach involves mechanical repositioning of the feed antenna or its selection for beam scanning/switching, which adds complexity to the antenna structure or feed selection/switching mechanisms [22], [23], [24], [25], [26], [27].

In this letter, we present a novel strategy to simplify beam switching in TAs. Our approach seamlessly integrates feed antennas within the beam-focusing surface and uses microswitches for feed selection and beam switching. This innovative method not only simplifies the implementation process but also eliminates the need for specialized supporting structures, leading to a more streamlined and efficient TA design. By embedding the switchable feed antenna directly into the beam-focusing surface and adding a reflector, we effectively halve the antenna's size in the boresight direction, which is a significant advancement over traditional designs that require separate feed antennas and complex supporting frameworks. This compact and efficient design is particularly advantageous for applications where space and ease of installation are critical considerations.

The proposed antenna is well suited for a variety of applications, including:

- *Vehicular radar systems:* The low-profile and beam-switching capabilities make it ideal for integration into vehicles where space is limited, and dynamic beam steering is essential for adaptive cruise control and collision avoidance systems.
- *Wireless communication networks:* The ability to switch beams rapidly and accurately can enhance the performance of wireless communication systems, particularly in dense urban environments where maintaining a reliable signal is challenging.
- *Industrial automation:* In industrial settings, where equipment and machinery need precise and reliable communication links, the compact size and robust performance of this antenna can improve system efficiency and safety.
- *Medical devices:* For medical imaging and therapeutic applications operating in the ISM band, the antenna's compact form factor and high precision can lead to better patient outcomes and more efficient diagnostic processes.

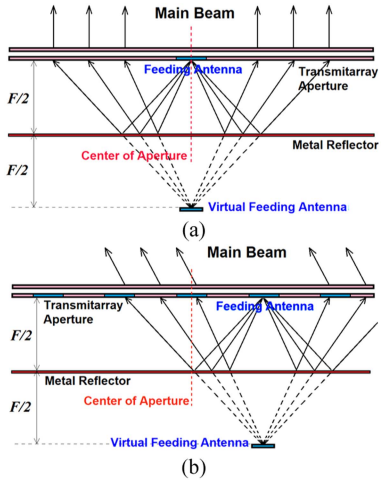

Fig. 1. Proposed compact TA. (a) Boresight main beam (central feeding patch antenna). (b) Tilted main beam (noncentral feeding patch antenna).

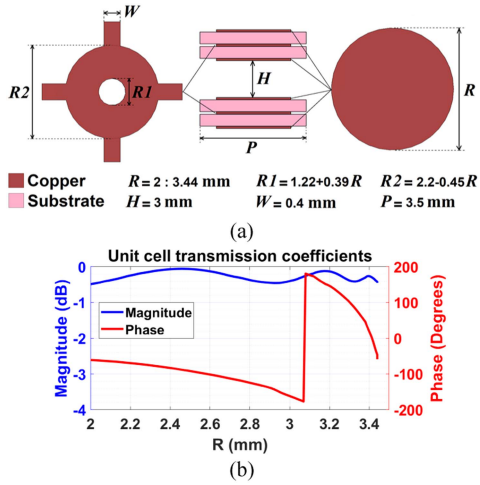

Fig. 2. Unit cell: (a) configuration and parameters and (b) transmission coefficients in terms of R at 24.125 GHz (R is swept from 2.00 to 3.44 mm).

Overall, the proposed TA design offers a highly practical solution for modern applications requiring compact, low-profile, and efficient beam-switching antennas.

The rest of this letter is organized as follows. Section II presents an integrated design of a highly low-profile TA; Section III details the used unit cell, the patch antenna that serves as a feed, and the switching system; Section IV presents the proposed TA, and Section V concludes the letter.

II. Integrated Design of Low-Profile TA

Our proposed TA structure, illustrated in Fig. 1, embeds the feed antenna into the beam-focusing surface and uses a reflector to redirect the radiated beam. This innovative design effectively reduces the antenna's size in the boresight direction by half, overcoming the limitations of traditional TAs that require separate feed antennas and complex supporting structures. While this method has been employed previously [28], [29], the novelty lies in designing and manufacturing a feed antenna and switching network that is fully integrated into the TA surface, eliminating the need for a separate and complex structure. In previously reported cases, a distinctly separate feed antenna was designed and manufactured, increasing construction complexities. Additionally, these designs typically employ only one feed antenna, lacking the capability of beam switching. Furthermore, to reduce the *F/D* ratio, a metallic reflector surrounding the patch antenna is not used. Consequently, by considering $F/D = 0.5$ in the design, the distance between the metal reflector and the TA surface is reduced to $D/4$ (where F and D are the focal point and the largest dimensions of the TA, respectively).

In the feed antenna design, two challenges were tackled. The first challenge was to enable the simultaneous fabrication of the feed antenna and the TA surface using printed circuit board (PCB) technology. This required the unit cell and feed antenna to be designed with the same substrate. The second challenge was to enable beam switching, which required multiple patch antennas on the TA surface [Fig. 1(b)]. However, this resulted in a decrease in the effective surface area for beam focusing. Therefore, the patch feed antennas needed to be arranged and switched with minimal space usage. To achieve this, we utilized MASW-011199 switch [30] along with a coplanar waveguide with ground (CPWG) lines. Section III provides detailed explanations of the design specifics for each component.

III. Unit Cell, Patch Antenna, and Switching System

In the design of the unit cell and patch antenna for feeding, we drew upon our prior expertise [26], with the key difference being that the design and optimization were centered around a center frequency of 24.125 GHz. Additionally, to ensure a low-profile TA and the simultaneous fabrication of the TA surface and the patch antennas on a single PCB, the patch antenna, akin to the unit cell, was engineered on a Taconic substrate with a permittivity of $\varepsilon_r = 3.43$, dielectric loss tangent of $\tan \delta = 0.0018$, and a thickness of 0.254 mm.

Fig. 2(a) displays the layout and parameters of the unit cell employed in this study. We simulated the transmission coefficients of the unit cell using CST Microwave Studio software [31], applying periodic boundary conditions and radiating a plane wave from top to bottom [Fig. 2(b)]. As illustrated, the unit cell successfully achieved a complete 360° phase shift at 24.125 GHz, accompanied by a transmission magnitude loss of less than 0.5 dB.

Fig. 3(a) illustrates the configuration of the patch antenna designed to illuminate the TA aperture. The patch is fed through U-shaped slots in the center ground plane and has been optimized to enhance antenna performance at 24.125 GHz. The simulated results of *S*-parameters and radiation patterns are illustrated in Fig. 3(b) and (c), respectively.

As previously stated, to achieve beam-switching capability, we utilized MASW-011199 switches along with CPWG lines to feed the patch antennas. For accurate testing and to achieve suitable matching, we initially designed and optimized a separate evaluation board with the desired substrate for the switch. Fig. 4 shows the produced board and the test results. As can be seen, the circuit exhibits proper matching, with transmission losses aligning well with the switch datasheet (the measured transmission losses for output ports 2–5 are 2.74 dB, 2.15 dB, 2.34 dB, and

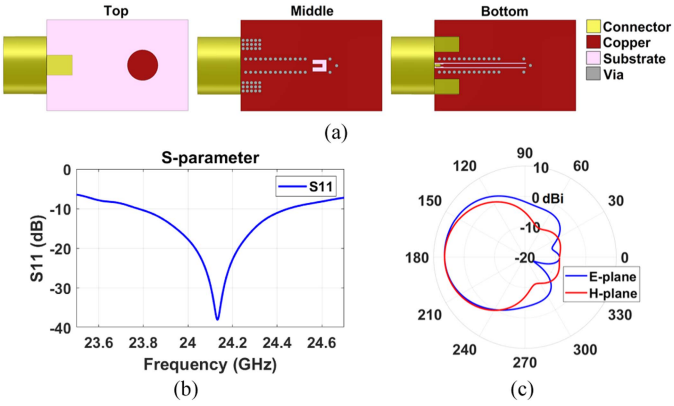

Fig. 3. Feeding patch antenna: (a) configuration of antenna, (b) simulated S-parameters results, and (c) simulated radiation patterns at E-plane and H-plane at 24.125 GHz.

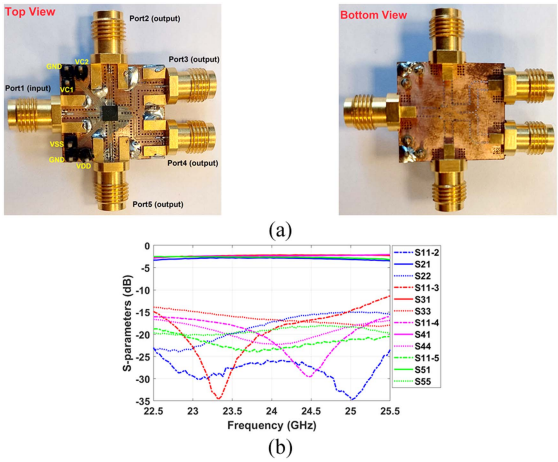

Fig. 4. MASW-011199 switch evaluation board: (a) fabricated and (b) measured results.

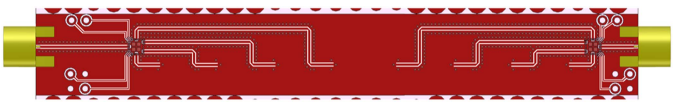

Fig. 5. Feeding network of antennas with switching capability.

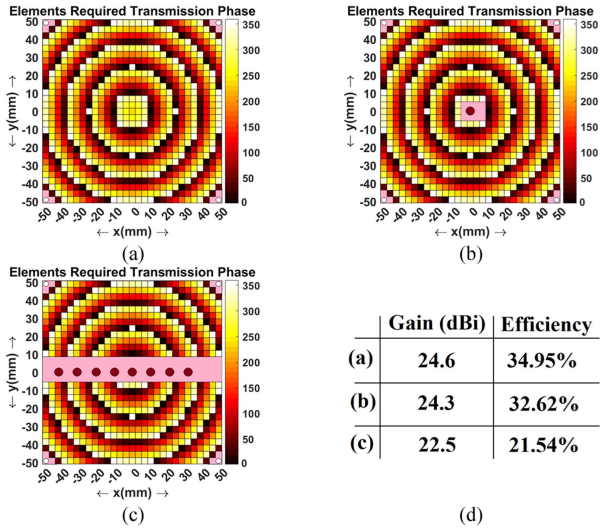

	Gain (dBi)	Efficiency
(a)	24.6	34.95%
(b)	24.3	32.62%
(c)	22.5	21.54%

(d)

Fig. 6. Various scenarios of simulated TA for the boresight direction of the main beam: (a) conventional TA, (b) 12 central cells are replaced with feeding patch antenna, (c) 116 central cells are replaced with feeding patch antennas, and (d) gain and efficiency of the antennas (boresight direction).

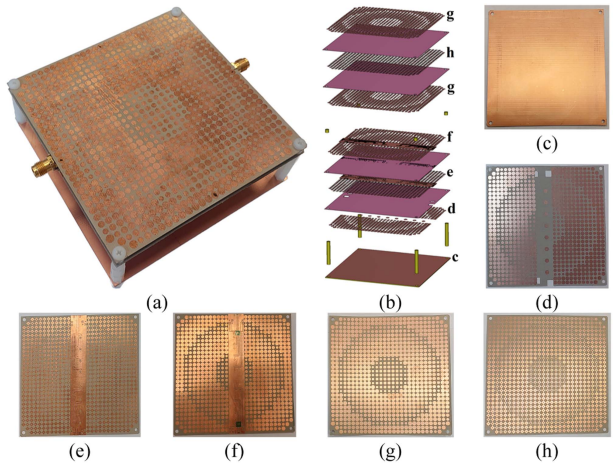

Fig. 7. Proposed TA: (a) fabricated TA, (b) the exploded view, (c) reflector, (d) top of first board, (e) middle of first board, (f) bottom of first board, (g) top and bottom of second board, and (h) middle of the second board.

2.53 dB at the frequency of 24.125 GHz, respectively). However, some variations in the results across different output ports are noted, which could be attributed to manufacturing and assembly discrepancies. Fig. 5 shows the feeding network of antennas with switching capability. As seen in the figure, each group of four antennas is fed by one port and controlled by one switch.

IV. Compact Beam-Switchable Transmitarray Antenna

A TA, consisting of 829 unit cells and measuring 101.5 mm by 101.5 mm ($8.16\lambda_0 \times 8.16\lambda_0$) for a central frequency of 24.125 GHz with an *F/D* ratio of 0.5, has been designed. Fig. 6 illustrates the phase distribution on the antenna surface and provides simulation results for various scenarios in the boresight direction of the main beam. In the first scenario, a conventional TA is employed with the feed antenna located at the focal point (*F*). The second scenario involves replacing 12 central cells (3×4) on the TA surface with a feeding patch antenna, and placing a reflector at an *F*/2 distance. As observed, there is an acceptable reduction of approximately 0.3 dB in antenna gain. The third scenario aims to investigate the impact of adding extra patch antennas to achieve beam-switching capability on the antenna. For this we removed 116 central cells (29×4) and placed the patch antennas at the center of the surface. In this case, beam-switching capability is attained at a cost of around 2.1 dB of antenna gain.

Fig. 7 illustrates the constructed antenna along with the constituent surfaces. As observed, the antenna does not require a specific supporting structure. Instead, the surfaces are simply connected to each other using four plastic supports. Moreover, the feed patch antenna is designed on the board related to the beam-focusing surface, making its fabrication very convenient using PCB technology. As seen in the figures, eight patch antennas are used for feeding. The central antenna, along with three others on the positive *X*-axis, is fed using one switch and

TABLE I
COMPARISON OF THE PROPOSED TA WITH SOME REFERENCES IN BEAM-SCANNING ANTENNAS

Ref.	Freq. [GHz]	Gain [dBi]	Feed Antenna(s)	Beam Scanning Technology	Using one PCB for antenna aperture and unit-cells	Total height of the antenna	Scan Range	Aperture Efficiency	3dB-gain bandwidth
[22]	10	25.6	Phased array	Selecting the feed	No	0.375D	±30°	57.5%	--
[23]	25	29.4	Horn	Moving the feed	No	0.5D	±30°	25%	>15.4%
[24]	27	18.5	Dipole	Selecting the feed	No	0.44D	±33°	24.8%	33.3%
[25]	30	28.8	Horn	Moving the feed	No	D	±18°	41.9%	34.8%
[26]	28	21.4	Patch	Selecting the feed	No	0.42D	±30°	36.8%	7.2%
This study	24.125	19.85	Patch	Switching System	Yes	0.25D	-24° / +32°	11.7%	5.1%

*The gains, aperture efficiencies, and gain bandwidths are based on the boresight beam.

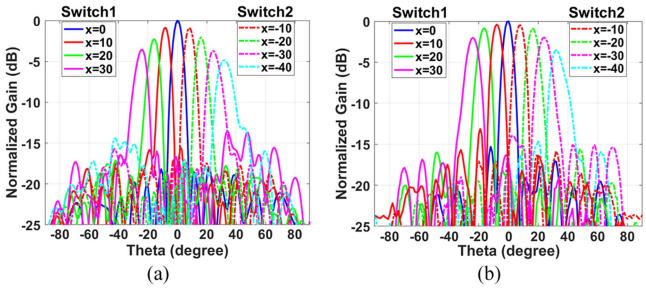

Fig. 8. Normalized radiation pattern of the TA antenna at 24.125 GHz: (a) simulated and (b) measured.

port, and the remaining four antennas on the negative X-axis are fed using a second switch and port. The distance between the patches is 10 mm, equivalent to an 8° tilt in the antenna beam. Therefore, the antenna, in addition to boresight direction, has the capability of beam switching at angles of 8°, 16°, and 24° in the negative X-axis direction and angles of 8°, 16°, 24°, and 32° in the positive X-axis direction. Because our goal was to have a beam in the boresight direction to compare with other tilts, we placed a patch antenna in the center of the aperture. Consequently, the arrangement of the other patch antennas is not symmetrical with respect to the aperture (three antennas in the positive direction and four antennas in the negative direction). As a result, the number of beams differs in the two directions of the x-axis (three beams in the negative direction and four beams in the positive direction). Depending on the application, the antennas can be placed symmetrically with respect to the aperture and have beams tilted at 4°, 12°, 20°, and 28° in both the positive and negative directions (with no boresight beam).

Fig. 8 shows both the simulation and measured results of the normalized radiation pattern of the antenna. As observed, the simulation and measured results align well. The maximum measured antenna gain was 19.85 dBi, and a tilt of 32° was achieved with a gain reduction of approximately 3.52 dB compared to the boresight condition. The comparison of simulated and measured gains shows a notable difference: the maximum simulated gain was 22.5 dBi, while the measured gain was 19.85 dBi. This discrepancy is mainly due to losses from the switch and feeding path. In simulations, each antenna was directly fed without accounting for losses, whereas the actual feeding network had longer paths for the middle antennas, resulting in greater losses compared to the corner antennas. Consequently, the measured gain for the boresight beam is further reduced, leading to lower gain roll-off. As mentioned earlier, our primary objective was to construct a highly low-profile antenna. Naturally, techniques to minimize side lobe levels and gain roll-off can be implemented in this design.

Table I presents a comparison between the proposed TA and similar beam-scanning antennas from the literature. The aperture efficiency in the table is calculated using the following equations:

$$\eta_{ap} = \frac{G}{D_{\max}}, \quad D_{\max} = \frac{4\pi A}{{\lambda_0}^2} \tag{1}$$

where G is the measured gain, $D_{\max}$ is the maximum directivity, A is the area of the antenna aperture, and λ_0 is the free-space wavelength.

Several conclusions can be drawn based on the data provided in Table I. First, the proposed antenna is the first to employ both the feed antennas and unit cells on a single PCB, simplifying its manufacturing. Additionally, it uses a switching system for beam steering. Due to its structure and the use of a reflector, it has the lowest height compared to other designs. The antenna has a lower efficiency compared to others. Part of this is due to the placement of the feed antennas in the antenna aperture, as explained in Fig. 6. The major part of the decrease in efficiency is due to the loss caused by the switch in the feeding path. It should be noted that other antennas require an external feeding network to select the feed antenna, which itself causes losses and reduces the overall efficiency of the antenna. However, the proposed antenna eliminates the need for a separate feeding network. Also, the lower gain bandwidth of the proposed antenna, compared to others, is due to the use of a patch antenna as the feed, which is narrowband at the designed operating frequency.

V. CONCLUSION

This letter introduces a novel state-of-the-art, ultralow-profile TA for the 24 GHz ISM band. The design is innovative, embedding the switchable feed antenna into the beam-focusing surface, which effectively halves the boresight dimensions. This makes it particularly suitable for vehicular radar applications. A standout feature of this design is the microswitch-enabled beam switching. The TA, consisting of 829 units and an F/D ratio of 0.5, demonstrates remarkable beam-switching. It can switch at angles of 8°, 16°, and 24° in the negative X-axis, and 8°, 16°, 24°, and 32° in the positive X-axis, alongside boresight direction. Operating at 24.125 GHz, the antenna achieves a maximum gain of 19.85 dBi, featuring a 32° tilt with a 3.52 dB gain reduction compared to the boresight condition.

REFERENCES

[1] J. Wang et al., "Compact wideband circularly-polarized mechanically beam-steering antenna for Ka-band vehicular communications," *IEEE Trans. Veh. Technol.*, vol. 73, no. 3, pp. 3393–3403, Mar. 2024.

[2] A. Papathanasopoulos and Y. Rahmat-Samii, "Transmitarray antenna for conical beam scanning," *IEEE Trans. Antennas Propag.*, vol. 70, no. 11, pp. 11155–11160, Nov. 2022.

[3] W. Hu et al., "Low-cost wide-angle beam-scanning transmitarray antennas using lens-loaded patch elements: A proof-of-concept study," *IEEE Antennas Wireless Propag. Lett.*, vol. 21, no. 12, pp. 2552–2556, Dec. 2022.

[4] H. Lei et al., "A low-profile risley-prism-based 2-D beam-scanning circularly polarized folded transmitarray antenna at Ku-band," *IEEE Trans. Antennas Propag.*, vol. 71, no. 7, pp. 6173–6178, Jul. 2023.

[5] Z. Zhai, F. Lin, Y. Yang, and H. Sun, "Additively manufactured wideband low-profile bidirectional 2-D beam-scanning antenna using double folded transmitarrays with curved polarizers," *IEEE Trans. Antennas Propag.*, vol. 72, no. 1, pp. 476–486, Jan. 2024.

[6] L. Z. Song, P. Y. Qin, H. Zhu, and J. Du, "Wideband conformal transmitarrays for E-band multi-beam applications," *IEEE Trans. Antennas Propag.*, vol. 70, no. 11, pp. 10417–10425, Nov. 2022.

[7] P. Y. Qin, L. Z. Song, and Y. J. Guo, "Conformal transmitarrays for unmanned aerial vehicles aided 6G networks," *IEEE Commun. Mag.*, vol. 60, no. 1, pp. 14–20, Jan. 2022.

[8] P. Y. Qin, L. Z. Song, and Y. J. Guo, "Beam steering conformal transmitarray employing ultra-thin triple-layer slot elements," *IEEE Trans. Antennas Propag.*, vol. 67, no. 8, pp. 5390–5398, Aug. 2019.

[9] S. H. R. Tuloti, P. Rezaei, and F. T. Hamedani, "High-efficient wideband transmitarray antenna," *IEEE Antennas Wireless Propag. Lett.*, vol. 17, no. 5, pp. 817–820, May 2018.

[10] S. H. Ramazannia Tuloti, Z. Mousavirazi, A. Kesavan, and T. A. Denidni, "A low profile dual-polarized transmitarray antenna at Ka-band," *AEU - Int. J. Electron. Commun.*, vol. 143, Jan. 2022, Art. no. 154016.

[11] T. K. Pham, L. Guang, D. González-Ovejero, and R. Sauleau, "Dual-band transmitarray with low scan loss for Satcom applications," *IEEE Trans. Antennas Propag.*, vol. 69, no. 3, pp. 1775–1780, Mar. 2021.

[12] S. H. Ramazannia Tuloti, P. Rezaei, and F. T. Hamedani, "Unit cell with flexible transmission phase slope for ultra-wideband transmitarray antennas," *Microw., Antennas Propag.*, vol. 13, no. 10, pp. 1522–1528, Aug. 2019.

[13] C. Huang, W. Pan, and X. Luo, "Low-loss circularly polarized transmitarray for beam steering application," *IEEE Trans. Antennas Propag.*, vol. 64, no. 10, pp. 4471–4476, Oct. 2016.

[14] Y. Wang, S. Xu, F. Yang, and M. Li, "A novel 1 bit wide-angle beam scanning reconfigurable transmitarray antenna using an equivalent magnetic dipole element," *IEEE Trans. Antennas Propag.*, vol. 68, no. 7, pp. 5691–5695, Jul. 2020.

[15] X. Wang, P. Y. Qin, A. Tuyen Le, H. Zhang, R. Jin, and Y. J. Guo, "Beam scanning transmitarray employing reconfigurable dual-layer Huygens element," *IEEE Trans. Antennas Propag.*, vol. 70, no. 9, pp. 7491–7500, Sep. 2022.

[16] L. Di Palma, A. Clemente, L. Dussopt, R. Sauleau, P. Potier, and P. Pouliguen, "Circularly-polarized reconfigurable transmitarray in Ka-band with beam scanning and polarization switching capabilities," *IEEE Trans. Antennas Propag.*, vol. 65, no. 2, pp. 529–540, Feb. 2017.

[17] J. Tang, S. Xu, F. Yang, and M. Li, "Design and measurement of a reconfigurable transmitarray antenna with compact varactor-based phase shifters," *IEEE Antennas Wireless Propag. Lett.*, vol. 20, no. 10, pp. 1998–2002, Oct. 2021.

[18] T. J. Li, G. M. Wang, W. L. Guo, K. W. Xin, J. Q. Han, and H. P. Li, "Reconfigurable folded transmitarray antenna with low-profile based on metasurfaces," *IEEE Antennas Wireless Propag. Lett.*, vol. 22, no. 3, pp. 611–615, Mar. 2023.

[19] A. R. Vilenskiy, M. N. Makurin, C. Lee, and M. V. Ivashina, "Reconfigurable transmitarray with near-field coupling to gap waveguide array antenna for efficient 2-D beam steering," *IEEE Trans. Antennas Propag.*, vol. 68, no. 12, pp. 7854–7865, Dec. 2020.

[20] B. Xi, Y. Xiao, H. Dong, M. Xiang, F. Yang, and Z. Chen, "Low-profile wideband 1-bit reconfigurable transmitarray with 2-D beam-scanning capacity," *IEEE Trans. Antennas Propag.*, vol. 71, no. 4, pp. 3228–3237, Apr. 2023.

[21] J. R. Reis, R. F. S. Caldeirinha, A. Hammoudeh, and N. Copner, "Electronically reconfigurable FSS-inspired transmitarray for 2-D beamsteering," *IEEE Trans. Antennas Propag.*, vol. 65, no. 9, pp. 4880–4885, Sep. 2017.

[22] P. Y. Feng, S. W. Qu, and S. Yang, "Phased transmitarray antennas for 1-D beam scanning," *IEEE Antennas Wireless Propag. Lett.*, vol. 18, no. 2, pp. 358–362, Feb. 2019.

[23] P. Mei, G. F. Pedersen, and S. Zhang, "Performance improvement of mechanically beam-steerable transmitarray antennas by using offset unifocal phase symmetry," *IEEE Trans. Antennas Propag.*, vol. 71, no. 1, pp. 1129–1134, Jan. 2023.

[24] J. Hu, H. Wong, and L. Ge, "A circularly-polarized multi-beam magneto-electric dipole transmitarray with linearly-polarized feeds for millimeter-wave applications," *IEEE Trans. Antennas Propag.*, vol. 70, no. 7, pp. 6012–6017, Jul. 2022.

[25] X. Wang, Y. Cheng, and Y. Dong, "Millimeter-wave dual-polarized metal transmitarray antenna with wide gain bandwidth," *IEEE Antennas Wireless Propag. Lett.*, vol. 21, no. 2, pp. 381–385, Feb. 2022.

[26] S. H. R. Tuloti, A. Lamecki, and M. Mrozowski, "An optimized Ka-band low profile dual-polarized transmitarray antenna with 2D beam switching," *IEEE Access*, vol. 12, pp. 8924–8931, 2024.

[27] J. Ala-Laurinaho, A. Karttunen, J. Säily, A. Lamminen, R. Sauleau, and A. V. Räisänen, "MM-wave lens antenna with an integrated LTCC feed array for beam steering," in *Proc. 4th Eur. Conf. Antennas Propag.*, Barcelona, Spain, 2010, pp. 1–5.

[28] P. Mei, S. Zhang, and G. F. Pedersen, "A low-profile and beam-steerable transmitarray antenna: Design, fabrication, and measurement [Antenna Applications Corner]," IEEE Antennas Propag. Mag., vol. 63, no. 5, Oct. 2021.

[29] P. Mei, S. Zhang, and G. F. Pedersen, "A dual-polarized and high-gain X-/Ka-band shared-aperture antenna with high aperture reuse efficiency," *IEEE Trans. Antennas Propag.*, vol. 69, no. 3, pp. 1334–1344, Mar. 2021.

[30] "[Online]. Available: https://cdn.macom.com/datasheets/MASW-011199.pdf"

[31] "Dassault Systèmes, Vélizy-Villacoublay, France," Jun. 3, 2022. CST Microwave Studio. Release Version 2022.05. [Online]. Available: http://www.cst.com